Usefulness of entanglement-assisted quantum metrology

Zixin Huang,[1] Chiara Macchiavello,[2] and Lorenzo Maccone[2]
[1]*School of Physics, The University of Sydney, Sydney, NSW 2006, Australia*
[2]*Dipartimento Fisica "A. Volta" and INFN Sezione Pavia, University of Pavia, via Bassi 6, I-27100 Pavia, Italy*
(Received 31 March 2016; published 1 July 2016)

Entanglement-assisted quantum communication employs preshared entanglement between sender and receiver as a resource. We apply the same framework to quantum metrology, introducing shared entanglement between the probe and the ancilla in the preparation stage and allowing entangling operations at the measurement stage, i.e., using some entangled ancillary system that does not interact with the system to be sampled. This is known to be useless in the noiseless case, but was recently shown to be useful in the presence of noise [R. Demkowicz-Dobrzanski and L. Maccone, Phys. Rev. Lett. **113**, 250801 (2014); W. Dür, M. Skotiniotis, F. Fröwis, and B. Kraus, *ibid.* **112**, 080801 (2014); E. M. Kessler, I. Lovchinsky, A. O. Sushkov, and M. D. Lukin, *ibid.* **112**, 150802 (2014); R. Demkowicz-Dobrzański and J. Kolodynski, New J. Phys. **15**, 073043 (2013)]. Here we detail how and when it can be of use. For example, surprisingly it is useful when two channels are randomly alternated, for both of which ancillas do not help (depolarizing). We show that it is useful for all levels of noise for many noise models and propose a simple optical experiment to test these results.

DOI: 10.1103/PhysRevA.94.012101

Entanglement-assisted communication [1–3] employs preshared entanglement between sender and receiver in addition to the signals sent through the channel. This doubles the capacity of a noiseless channel, as illustrated in the well-known superdense coding protocol [1], and is even more beneficial in the presence of noise [3,4]. Here we apply the same framework to quantum metrology [5–9], which studies how quantum effects may aid parameter estimation.

A quantum parameter estimation is composed of three stages [Fig. 1(a)]: the preparation stage, some probe systems are initialized; the sampling stage, the probes interact with the system to be sampled (this interaction encodes the parameter on the probes); and the measurement stage, the probes are measured and the outcome is processed to yield the parameter estimate. Entanglement-assisted quantum metrology [Fig. 1(b)] refers to the scenario in which the probes are entangled with an ancilla that does not participate in the sampling stage (similar ideas have also been studied in the context of noisy channel estimation [10,11]). Then at the measurement stage a joint measurement is performed between probes and the ancilla. It was recently realized that this is useful in the presence of noise [12–17], although it was known to be useless in the noiseless case [5]. Here we detail how entangled ancillas can be used, what are the gains one can achieve, and which explicit measurement strategies can achieve such gains, analyzing the most important qubit channels. We also propose a simple experiment that can test our results.

The entanglement-assisted scenario should not be confused with the generic use of entanglement in quantum estimation, which has been extensively studied previously, e.g., see Refs. [5,18–26], showing how entangled probes achieve better precision than unentangled ones. It is also different from the application of quantum error correction (QEC) to metrology [13–15,27] where all the systems are involved in the interaction [Fig. 1(c)], although some scenarios analyzed in Refs. [13–15,27] go beyond this conventional quantum error correction scheme. Instead, in the entanglement-assisted scenario, the ancilla does not interact and can be considered as noiseless, if we suppose (as is often the case) that the noise is relevant especially during the interaction stage. This translates into a reduced noise acting on the global state and a reduced resource count: indeed in quantum metrology the resource count most commonly refers to the number of times that the probed system is sampled [8]. So, the entangled ancillas should be accounted for as separate resources, as is done in quantum communication [1–3]. Clearly this resource accounting is not appropriate for all scenarios, and the "cost" of entangled ancillas may be significant in certain implementations.

We detail the increase in achievable precision in the presence of an entangled ancilla with respect to the one achievable in its absence, instead of dealing with the issue of whether one can beat the standard quantum limit or achieve the Heisenberg bound. Indeed, it is known that the Heisenberg scaling cannot be achieved asymptotically for many of these noise models [28–32], although it can often be achieved in the nonasymptotic regime [33–35]. Interestingly, it has been pointed out [13–15] that the Heisenberg scaling *can* be recovered through entanglement-assisted metrology even asymptotically in the very special case of orthogonal noise, even though only a lower scaling is achieved in the absence of ancillas [25]. However a general analysis of entanglement-assisted metrology has been lacking up to now: our results show the attainable precision enhancement for the case of the Pauli channels (including the fully depolarizing case) and of the amplitude damping. Moreover, dephasing and erasure noise do not allow for any enhancement in the entanglement-assisted scenario, although entanglement among the probes is helpful [12].

Most previous literature studies the precision through the quantum Cramer-Rao (QCR) bound, with the promise that such a lower bound to precision is significant because it is asymptotically achievable. However, since we want achievability in the nonasymptotic regime, we must provide estimation strategies and prove that they achieve the QCR, at least in a feedback scenario [36,37]. Indeed, both the QCR and the error in the employed strategy may depend on the unknown parameter to be estimated [38], but a feedback

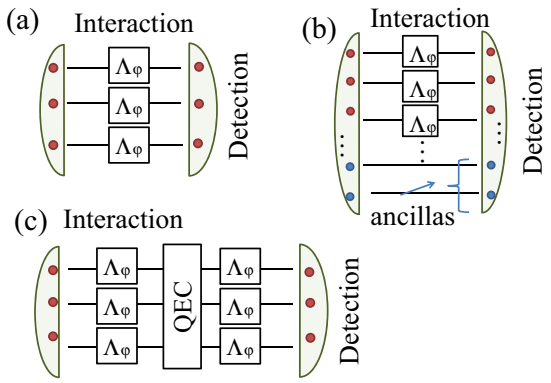

FIG. 1. (a) Conventional quantum parameter estimation: Probes are prepared in a joint entangled state, they interact (independently) with the probed system through a noisy map Λ_φ, and they are jointly measured. (b) Entanglement-assisted parameter estimation: Ancillary systems are employed that do not interact with the probed system. (c) Quantum error correction schemes: After the interaction the errors are corrected and, possibly, the probes interact again.

strategy converges exponentially to the "sweet spot" [39], so that it has only a logarithmic cost in terms of resources [36]. Even though the rigorous way to determine phase errors is the Holevo variance [40,41], as is usually done in the literature we use the customary variance, since the two match for sufficiently precise estimation strategies.

The QCR [18,19,40,42] is a lower bound to the precision $\Delta\varphi$ of the estimation of a parameter φ: under reasonable hypotheses, $\Delta\varphi \geqslant 1/\sqrt{\nu J(\rho_\varphi)}$, where ν is the number of times the estimation is repeated and J is the quantum Fisher information (QFI) associated with the global state ρ_φ of probes and ancillas (after the interaction Λ_φ with the probed system). The QFI is

$$J(\rho_\varphi) = \sum_{j,k:\lambda_j+\lambda_k\neq 0} 2|\langle j|\rho'_\varphi|k\rangle|^2/(\lambda_j+\lambda_k), \qquad (1)$$

where $\rho'_\varphi = \partial\rho_\varphi/\partial\varphi$, and λ_j and $|j\rangle$ are the eigenvalues and eigenvectors of ρ_φ. The map Λ_φ encodes the phase parameter φ onto the probes: $\rho_\varphi = \Lambda_\varphi[\rho]$, ρ being the initial state. Without loss of generality, for qubit channels we suppose that the phase is encoded onto the computational basis by the unitary $U_\varphi = |0\rangle\langle 0| + e^{i\varphi}|1\rangle\langle 1|$. For the sake of simplicity we consider situations where the noise map $\mathcal{E}$ acts after U_φ, namely $\Lambda_\varphi = \mathcal{E}\circ U_\varphi$. If the noise map and U_φ do not commute, this is an important restriction of our analysis (required to make the problem tractable, as nontrivial effects arise otherwise [25]), but it is not a restriction for the erasure, amplitude-damping, and depolarizing noise models which commute with U_φ.

To find the best bound, one must maximize the QFI, which in general depends both on the input state ρ and on the unknown parameter φ. The former optimization depends on the noise map; the latter can be taken care of using feedback mechanisms [36–39]. For all noise maps, we can use the convexity of the QFI [10] to choose a pure input state $\rho = |\psi\rangle\langle\psi|$. Indeed, supposing that $\rho = \sum_j \lambda_j |j\rangle\langle j|$, we have $J(\rho_\varphi) = J(\sum_j \lambda_j \Lambda_\varphi[|j\rangle\langle j|]) \leqslant \sum_j \lambda_j J(\Lambda_\varphi[|j\rangle\langle j|])$. (The QFI is not convex if λ_j depends on φ, but an extended convexity still holds [34].)

I. AMPLITUDE-DAMPING NOISE CHANNEL

We start by analyzing the amplitude-damping channel with Kraus operators

$$A_0 = \begin{pmatrix} 1 & 0 \\ 0 & \sqrt{1-\eta} \end{pmatrix}, \quad A_1 = \begin{pmatrix} 0 & \sqrt{\eta} \\ 0 & 0 \end{pmatrix}, \qquad (2)$$

where η is the probability of decay $|1\rangle \to |0\rangle$. This map is agnostic on the direction of the x and y axes of the Bloch sphere: a rotation around the z axis leaves A_0 unchanged and adds an inconsequential phase factor to A_1. Thus we can optimize the single-probe input state among the family $\epsilon|0\rangle + \sqrt{1-\epsilon^2}|1\rangle$. The optimal state has $\epsilon = 1/\sqrt{2}$, and its QFI is $1-\eta$. To show that entanglement-assisted strategies perform better, we compare this QFI with the one of an entangled state of the probe and the ancilla: $|\psi_\gamma\rangle = \gamma|00\rangle + \sqrt{1-\gamma^2}|11\rangle$. This state might not be the optimal state for the entanglement-assisted strategy, but it outperforms the previous one. Indeed its corresponding output state $(\Lambda_\varphi \otimes \mathbb{1})[|\psi_\gamma\rangle\langle\psi_\gamma|]$ (where the map acts only on the probe qubit and not on the ancilla) has a QFI of $4(1-\eta)/(\sqrt{1-\eta}+1)^2$ (shown by Ref. [17]), if one optimizes over γ for each η. Even the simple choice $\gamma = 1/\sqrt{2}$ is advantageous for all η as its QFI is $2(1-\eta)/(2-\eta)$. These QFIs are compared in Fig. 2(a).

An observable that achieves the QCR bound for the last QFI above (only asymptotically under an adaptive technique as discussed above) is $O = \Pi_\psi + 2\,|\Phi^+\rangle\langle\Phi^+|$, with $|\Phi^+\rangle = \frac{1}{\sqrt{2}}(|00\rangle + |11\rangle)$ and $\Pi_\psi = (|01\rangle\langle 01| + |10\rangle\langle 10|)$. Indeed, measuring the observable O, the error on φ is

$$\Delta\varphi^2 = \frac{\Delta O^2}{(d\langle O\rangle/d\varphi)^2} = \frac{1-\eta/2-(1-\eta)\cos^2\varphi}{(1-\eta)\sin^2\varphi}. \qquad (3)$$

This expression is optimized for $\varphi = \pi/2$, where the Cramer-Rao bound of the optimal single-probe state is beaten performing Bell measurements between the probe and the ancilla. As discussed above, we can perform the optimization $\varphi \to \pi/2$ using a feedback strategy [36–39], by introducing a known phase α and driving $\varphi+\alpha$ to $\pi/2$.

The ancilla-assisted advantage persists also when we use entangled probes. The case without ancillas is analyzed in Ref. [31] where an upper bound $N(1-\eta)/\eta$ to the Fisher information is given, N being the number of times the system is being sampled, which is achievable in the high-noise regime $N\eta/(1-\eta) \gg 1$.

In the case of two-qubit probes, one can also perform a numerical optimization of the QFI on generic two-qubit states $a\,|00\rangle + b\,|01\rangle + c\,|10\rangle + d\,|11\rangle$, where $|a|^2+|b|^2+|c|^2+|d|^2 = 1$ [presented in Fig. 2(b), solid line], where both qubits are probes. In this figure we compare strategies for when two probes sample the system, that is, using only two-qubit states to probe the system, or when the two probes are entangled to external ancillas.

Interestingly, the performance of the optimal state is similar to the that of the "NOON" state $|\Phi^+\rangle$, which is known to be optimal in the noiseless case. However, all these strategies can be beaten by using ancillas (as is noted also in Ref. [12], although

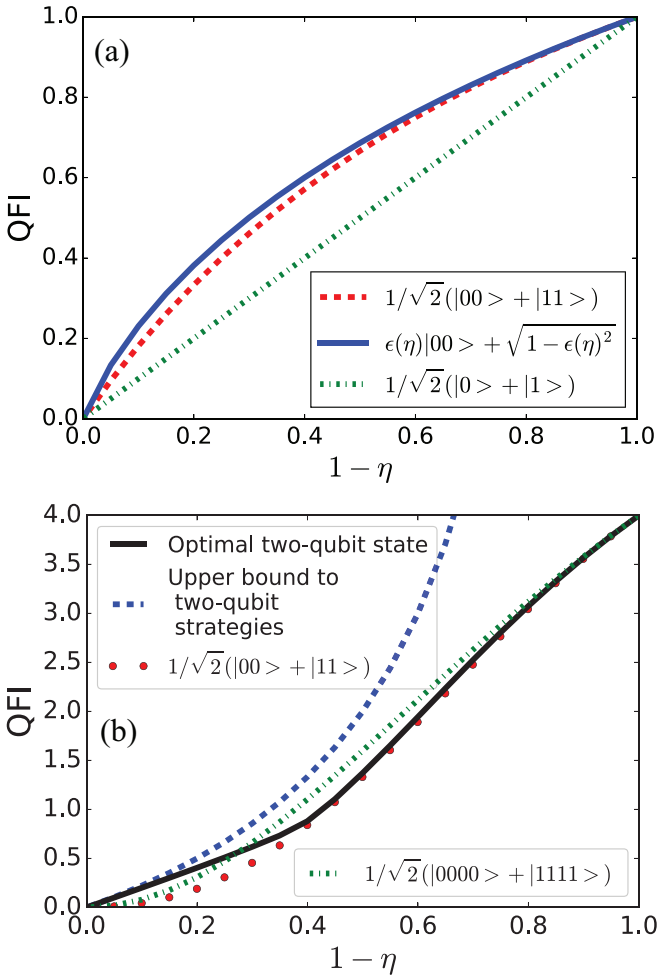

FIG. 2. (a) Single-qubit probe: QFI of the optimal ancilla-assisted state, $|\psi_\gamma\rangle = \epsilon(\eta)\,|00\rangle + \sqrt{1-\epsilon(\eta)^2}\,|11\rangle$ (continuous); the maximally entangled state of the probe and the ancilla, $\frac{1}{\sqrt{2}}(|00\rangle + |11\rangle)$ (dashed); and the unentangled single-qubit state, $\frac{1}{\sqrt{2}}(|0\rangle + |1\rangle)$, that is the probe (dotted). For all η the ancilla-assisted strategies have better QFI. (b) Two-qubit strategies: The optimal two-qubit state where both are probes (continuous line) and the two-qubit "NOON" state $[\frac{1}{\sqrt{2}}(|00\rangle + |11\rangle)$, both probes, optimal only in the noiseless case, red circles] are compared to a genuinely entangled four-qubit state $[\frac{1}{\sqrt{2}}(|0000\rangle + |1111\rangle)$, two probes and two ancilla qubits, dot-dashed line]. We also plot the upper bound to the ancillaless estimation with two probes from Ref. [31] (dashed), which is achievable in the high-noise regime (where the dashed and continuous lines superimpose). The ancilla-assisted strategy beats any entangled-probe strategies for $\eta < 0.7$. The state can be further optimized.

no explicit example is presented there). In Fig. 2(b), the dotted-dashed line, we show the performance of the four-qubit NOON state $(|0000\rangle + |1111\rangle)/\sqrt{2}$ of two probes and two ancillas: it beats the optimal state of two probes for noise levels $\eta \approx 0.7$, where its QFI is $\frac{8(\eta-1)^2\{2(\eta-1)^2\cos(8\varphi)+(\eta-2)\eta[(\eta-2)\eta+2]+2\}}{[(\eta-2)\eta+2]^3}$, which is optimal for $\varphi = \frac{2\pi n}{8}$, n being an integer. One observable that achieves the QCR for the single-qubit probe is $O{=}2\,|N\rangle\langle N| + \Sigma$, $|N\rangle = 1/\sqrt{2}(|0000\rangle - |1111\rangle)$, and $\Sigma{=}\,|0011\rangle\langle 0011| + |0111\rangle\langle 0111| + |1011\rangle\langle 1011|$. Note that this particular four-qubit state is not necessarily optimal.

II. GENERAL PAULI NOISE CHANNEL

The generalized Pauli noise channel channel is described by

$$\Lambda[\rho] = (1-p_1-p_2-p_3)\rho + p_1\sigma_x\rho\sigma_x^\dagger + p_2\sigma_y\rho\sigma_y^\dagger + p_3\sigma_z\rho\sigma_z^\dagger, \tag{4}$$

with σ_x, σ_y, and σ_z Pauli matrices and p_1, p_2, and p_3 probabilities. Two special Pauli channels are the dephasing noise and the depolarizing noise. Dephasing noise corresponds to $p_1 = p_2 = 0$ in Eq. (4) and it has been proven that ancillas offer no advantage over the unentangled probe [12]: for both cases the optimal QFI of a single-qubit probe is $(1-2p_3)^2$. Depolarizing noise corresponds to having $p_1 = p_2 = p_3 \equiv p/4$ in Eq. (4): it describes an isotropic loss of coherence. As is shown in Ref. [17], in this case ancillas do help: indeed for a single-qubit probe, the optimal state is $1/\sqrt{2}(|0\rangle + |1\rangle)$, where the QFI is $(1-p)^2$, whereas the QFI for a probe maximally entangled with an ancilla is $2(1-p)^2/(2-p)$, which is always greater .

This result is very surprising since the depolarizing channel can be seen as a noise map where with probability $1-p$ the channel remains noiseless, and in the other case the state of the probe is replaced by a maximally mixed state $\mathbb{1}/2$, which is useless for estimation. For both of these channels the use of an ancilla gives no advantage: the ancilla becomes important only when the channels are randomly alternated.

One observable that achieves the QCR for the single-qubit probe is $O = |+\rangle\langle+|$, $|+\rangle = 1/\sqrt{2}(|0\rangle + |1\rangle)$, and for the ancilla-assisted case, $O = \Pi_\psi + 2\,|\Phi^+\rangle\langle\Phi^+|$ (identical to the one for the amplitude-damping channel).

Even though dephasing and depolarizing channels commute with the unitary U_φ, in general the Pauli channel does not: we consider the case when the noise acts only after U_φ. For a single-qubit probe in the generic initial state $\epsilon|0\rangle + \sqrt{1-\epsilon^2}e^{i\alpha}|1\rangle$, the QFI is

$$\begin{aligned} J_\varphi^{(\mathrm{na})} = {} & 4\epsilon^2(\epsilon^2-1)\{p_1(2-4p_3) + 4p_3 - 4p_3(p_2+p_3) \\ & - 1 - 2{p_1}^2 - 2(-1+p_2)p_2 \\ & + 2(p_1-p_2)\cos[2(\alpha+\varphi)](p_1+p_2+2p_3-1)\} \end{aligned} \tag{5}$$

("na" stands for "no ancilla"), which is maximized for $\epsilon = 1/\sqrt{2}$ for all φ. As discussed previously, one can optimize over α using a feedback strategy. To prove that the presence of an ancilla is beneficial, we consider the maximally entangled state $\frac{1}{\sqrt{2}}(|00\rangle + |11\rangle)$ of the probe and the ancilla. In this case the QFI is

$$J_\varphi^{(a)} = \frac{(p_1-p_2)^2}{p_1+p_2} + \frac{(p_1+p_2+2p_3-1)^2}{1-p_1-p_2}. \tag{6}$$

We performed a numerical search over the parameter space p_1, p_2, p_3. For all possible values of $p_1 + p_2 + p_3 \leqslant 1$, the expression in Eq. (6) is larger than that in Eq. (5) for all α.

To illustrate this, the difference between Eqs. (6) and (5) is plotted in Fig. 3, for the case when $p_1{=}0$ and $\alpha{+}\varphi{=}0$. The probe-ancilla observable $\hat{O} = |\Phi^-\rangle\langle\Phi^-| + |\Psi^-\rangle\langle\Psi^-|$ achieves the QCR bound relative to the QFI of Eq. (6), with $|\Phi^-\rangle = \frac{1}{\sqrt{2}}(|00\rangle - |11\rangle)$ and $|\Psi^-\rangle = \frac{1}{\sqrt{2}}(|01\rangle - |10\rangle)$.

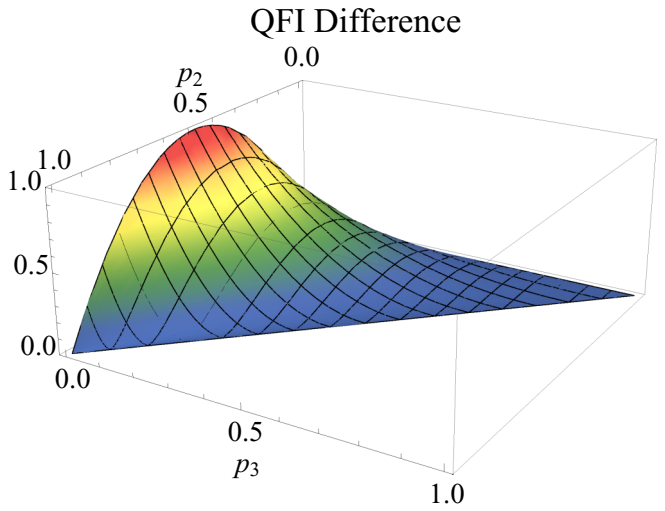

FIG. 3. General Pauli channel (for the case $p_1 = 0$). The difference between the ancilla-assisted strategy in Eq. (6) and the optimized QFI for a single probe in Eq. (5), Eq. (6)–Eq. (5), for $\epsilon = 1/\sqrt{2}$ and $\alpha + \varphi = 0$.

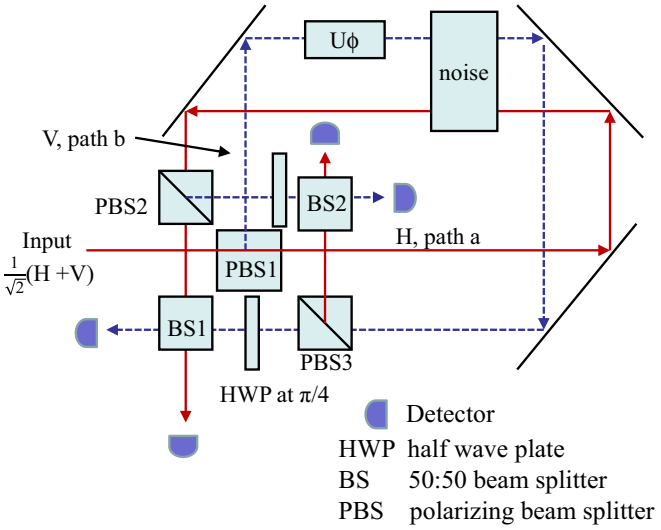

FIG. 4. An experimental scheme to perform phase estimations using the ancilla-assisted scheme. See text for details.

Note that, when $p_1(p_2) = 0$ and $p_1(p_2) + p_3 = 1$, the QFI is unity: this represents the case of orthogonal noise when the ancilla strategy can recover the full information on the phase even in the presence of noise, as is pointed out in Refs. [13–15].

III. EXPERIMENT PROPOSAL

We propose here an experimental scheme to implement our proposal, based on the use of a single photon, where two qubits are encoded in the path and the polarization degrees of freedom.

Such a scheme, which can simulate the ancilla-assisted strategy, is shown in Fig. 4. The experiment uses a single photon which is prepared in a polarization-path entangled state as follows and the noise acts on the polarization degree of freedom. The initial polarization state of the photon in this scheme is $\frac{1}{\sqrt{2}}(|H\rangle + |V\rangle)$. A polarizing beam splitter (PBS) then transmits $|H\rangle$ and reflects $|V\rangle$. Therefore, PBS1 acts as an effective CNOT gate and puts the initial state into a polarization-path entangled state $1/\sqrt{2}(|Ha\rangle + |Vb\rangle)$ (red solid arrow = a, blue dashed arrow = b). The state is then transformed according to the unitary U_φ and the noisy channel. Different noise models can be implemented, using liquid crystals [43] or wave plates. For example, the amplitude-damping channel can be implemented by placing a single half-wave plate (HWP) on path b where the angle of rotation with respect to the optic axis is mapped to the damping paramter γ; Pauli noises can be simulated by applying a combination of HWPs and quarter-wave plates across both paths a and b. If the bit is flipped, the flipped component is directed by PBS2 and PBS3 onto another path, which interfere at BS2. The HWP rotates V polarization to H so that they interfere at the 50:50 beam splitter (BS). The which-arm statistics after the BS are effective projective Bell measurements in this basis. That is, at BS1 the outputs correspond to projecting onto $1/\sqrt{2}(|Ha\rangle \pm |Vb\rangle)$, and at BS2 the outputs correspond to projecting onto $1/\sqrt{2}(|Va\rangle \pm |Hb\rangle)$. This scheme is easily implementable with present-day technologies, e.g., in Ref. [43] similar schemes are experimentally realized and controlled noise is introduced in an ancilla-assisted scenario for different purposes.

IV. CONCLUSIONS

In conclusion, we have studied the role of entangled ancillas in metrology for the important classes of qubit noise models. We have shown that, for a single probe, in the presence of amplitude-damping noise, depolarizing noise, and general Pauli noise, an entanglement-assisted scheme provides an advantage in the efficiency of phase measurement over the unentangled case for all ranges of noise regimes. We also derived the optimal measurement procedures which achieve the Cramer-Rao bound.

ACKNOWLEDGMENT

We acknowledge useful feedback from Rafal Demkowicz-Dobrzanski.

[1] C. H. Bennett and S. J. Wiesner, Phys. Rev. Lett. **69**, 2881 (1992).

[2] C. H. Bennett, P. W. Shor, J. A. Smolin, and A. V. Thapliyal, Phys. Rev. Lett. **83**, 3081 (1999).

[3] C. H. Bennett, P. W. Shor, J. A. Smolin, and A. V. Thapliyal, IEEE Trans. Inf. Theory **48**, 2637 (2002).

[4] Z. Shadman, H. Kampermann, C. Macchiavello, and D. Bruss, New J. Phys. **12**, 073042 (2010).

[5] V. Giovannetti, S. Lloyd, and L. Maccone, Phys. Rev. Lett. **96**, 010401 (2006).

[6] V. Giovannetti, S. Lloyd, and L. Maccone, Science **306**, 1330 (2004).

[7] W. van Dam, G. M. D'Ariano, A. Ekert, C. Macchiavello, and M. Mosca, Phys. Rev. Lett. **98**, 090501 (2007).

[8] V. Giovannetti, S. Lloyd, and L. Maccone, Nat. Photon. **5**, 222 (2011).

[9] J. P. Dowling, Contemp. Phys. **49**, 125 (2008).

[10] A. Fujiwara, Phys. Rev. A **63**, 042304 (2001); **70**, 012317 (2004).

[11] A. Fujiwara and H. Imai, J. Phys. A **36**, 8093 (2003).

[12] R. Demkowicz-Dobrzanski and L. Maccone, Phys. Rev. Lett. **113**, 250801 (2014).

[13] W. Dür, M. Skotiniotis, F. Fröwis, and B. Kraus, Phys. Rev. Lett. **112**, 080801 (2014).

[14] G. Arrad, Y. Vinkler, D. Aharonov, and A. Retzker, Phys. Rev. Lett. **112**, 150801 (2014).

[15] E. M. Kessler, I. Lovchinsky, A. O. Sushkov, and M. D. Lukin, Phys. Rev. Lett. **112**, 150802 (2014).

[16] S. A. Haine and S. S. Szigeti, Phys. Rev. A **92**, 032317 (2015); S. A. Haine, S. S. Szigeti, M. D. Lang, and C. M. Caves, *ibid.* **91**, 041802 (2015).

[17] R. Demkowicz-Dobrzański and J. Kolodynski, New J. Phys. **15**, 073043 (2013).

[18] S. L. Braunstein and C. M. Caves, Phys. Rev. Lett. **72**, 3439 (1994).

[19] S. L. Braunstein, C. M. Caves, and G. Milburn, Ann. Phys. **247**, 135 (1996).

[20] G. Y. Xiang, B. L. Higgins, D. W. Berry, H. M. Wiseman, and G. J. Pryde, Nat. Photon. **5**, 43 (2011).

[21] H. T. Dinani and D. W. Berry, Phys. Rev. A **90**, 023856 (2014).

[22] A. Shaji and C. M. Caves, Phys. Rev. A **76**, 032111 (2007).

[23] S. F. Huelga, C. Macchiavello, T. Pellizzari, A. K. Ekert, M. B. Plenio, and J. I. Cirac, Phys. Rev. Lett. **79**, 3865 (1997).

[24] M. Kacprowicz, R. Demkowicz-Dobrzanski, W. Wasilewski, K. Banaszek, and I. A. Walmsley, Nat. Photon. **4**, 357 (2010).

[25] R. Chaves, J. B. Brask, M. Markiewicz, J. Kolodyński, and A. Acín, Phys. Rev. Lett. **111**, 120401 (2013).

[26] L. Maccone and G. De Cillis, Phys. Rev. A **79**, 023812 (2009).

[27] R. Ozeri, arXiv:1310.3432.

[28] R. Demkowicz-Dobrzanski, J. Kolodynski, and M. Guta, Nat. Commun. **3**, 1063 (2012).

[29] B. Escher, R. de Matos Filho, and L. Davidovich, Nat. Phys. **7**, 406 (2011).

[30] M. Jarzyna and R. Demkowicz-Dobrzanski, New J. Phys. **17**, 013010 (2015).

[31] S. I. Knysh, E. H. Chen, and G. A. Durkin, arXiv:1402.0495.

[32] S. Alipour, M. Mehboudi, and A. T. Rezakhani, Phys. Rev. Lett. **112**, 120405 (2014).

[33] S. L. Braunstein, Phys. Rev. Lett. **69**, 3598 (1992).

[34] S. Alipour and A. T. Rezakhani, Phys. Rev. A **91**, 042104 (2015).

[35] R. Demkowicz-Dobrzanski, K. Banaszek, and R. Schnabel, Phys. Rev. A **88**, 041802(R) (2013).

[36] D. W. Berry and H. M. Wiseman, Phys. Rev. Lett. **85**, 5098 (2000); D. W. Berry, H. M. Wiseman, and J. K. Breslin, Phys. Rev. A **63**, 053804 (2001); D. Berry, arXiv:quant-ph/0202136.

[37] A. Hentschel and B. C. Sanders, Phys. Rev. Lett. **104**, 063603 (2010); **107**, 233601 (2011).

[38] G. A. Durkin and J. P. Dowling, Phys. Rev. Lett. **99**, 070801 (2007).

[39] K. P. Seshadreesan, S. Kim, J. P. Dowling, and H. Lee, Phys. Rev. A **87**, 043833 (2013).

[40] A. S. Holevo, *Probabilistic and Statistical Aspects of Quantum Theory* (North-Holland, Amsterdam, 1982).

[41] For the general case, see also G. M. D'Ariano, C. Macchiavello, and M. F. Sacchi, Phys. Lett. A **248**, 103 (1998).

[42] C. W. Helstrom, *Quantum Detection and Estimation Theory* (Academic Press, New York, 1976).

[43] A. Chiuri, V. Rosati, G. Vallone, S. Padua, H. Imai, S. Giacomini, C. Macchiavello, and P. Mataloni, Phys. Rev. Lett. **107**, 253602 (2011); A. Orieux, L. Sansoni, M. Persechino, P. Mataloni, M. Rossi, and C. Macchiavello, *ibid.* **111**, 220501 (2013); A. Orieux, M. A. Ciampini, P. Mataloni, D. Bruß, M. Rossi, and C. Macchiavello, *ibid.* **115**, 160503 (2015).